

Note

## Dense colloid transport in a bifurcating fracture

Scott C. James<sup>a,\*</sup> and Constantinos V. Chrysikopoulos<sup>b</sup>

<sup>a</sup> Sandia National Laboratories, Geohydrology Department, P.O. Box 5800, Albuquerque, NM 87185-0735, USA

<sup>b</sup> Department of Civil and Environmental Engineering, University of California, Irvine, CA 92697-2175, USA

Received 14 April 2003; accepted 6 September 2003

### Abstract

In this work, the transport of dense colloids through a water-saturated, bifurcating fracture is investigated using a constant spatial step particle tracking technique. The size of the constituents of a colloid plume is an important factor affecting the partitioning of dense colloids at the bifurcation. While neutrally buoyant colloids partition between daughter fractures in proportion to flow rates, dense colloids will preferentially exit fractures that are gravitationally downgradient, notwithstanding that the majority of the interstitial fluid may flow through the upper fracture. Comparison of the partitioning ratio between daughter fractures with the ratios of characteristic settling, diffusion, and advection time reveal that these parameters control how colloids behave at fracture bifurcations.

Published by Elsevier Inc.

*Keywords:* Dense colloid transport; Bifurcation; Fracture flow

### 1. Introduction

The term “fracture” is quite general and refers to various types of discontinuities (joints, fracture zones, and shear zones) that can break a subsurface medium into blocks. Fractures are found in almost all types of rocks: sedimentary (e.g., sandstone), metamorphic (e.g., limestone), and igneous or crystalline (e.g., granite). Naturally fractured systems contain extreme and abrupt changes in porosity and permeability and can be characterized by two distinct components, fractures and matrix blocks. Fractures are often the primary transmission conduits for fluids, colloids, and contaminants, and in many fractured systems, fracture bulk permeability exceeds matrix bulk permeability by several orders of magnitude [1].

In many geological formations with low matrix permeability, fluid flow predominantly takes place through a single fracture or fault, while in other cases the flow occurs through a network of fractures. Fracture networks comprise many individual fractures that intersect to some degree. Simulating fluid flow and contaminant transport in fractured subsurface formations with the intent of describing macroscale transport behavior often begins with modeling flow and transport

at the scale of an individual fracture [2–6]. As a basis for a comprehensive fracture network model, it is important to understand flow and transport through a single bifurcating fracture. In this work, colloid transport in a bifurcating fracture is modeled using a particle tracking technique. Simulations are conducted with varying geometric and physical parameters to discern how colloids will partition at a fracture intersection.

### 2. Model formulation

#### 2.1. Fracture system

The system considered in this work is composed of a parent fracture bifurcating into two daughter fractures as shown in Fig. 1. Heavier-than-water (dense) colloids are considered while colloid–colloid and colloid–wall interactions are neglected in this work. Changes in fluid viscosity and colloid diffusivity due to a concentrated suspension are neglected. As increased computing power becomes available, many more particles can be tracked, perhaps necessitating the inclusion of effective viscosities and diffusivities. The fracture walls are considered impermeable to both colloid transport and interstitial fluid flow. Unlike soluble contaminants, colloid particles are assumed to be too large to penetrate the rock matrix and therefore remain within the confines of the

\* Corresponding author.

E-mail address: [scjames@sandia.gov](mailto:scjames@sandia.gov) (S.C. James).

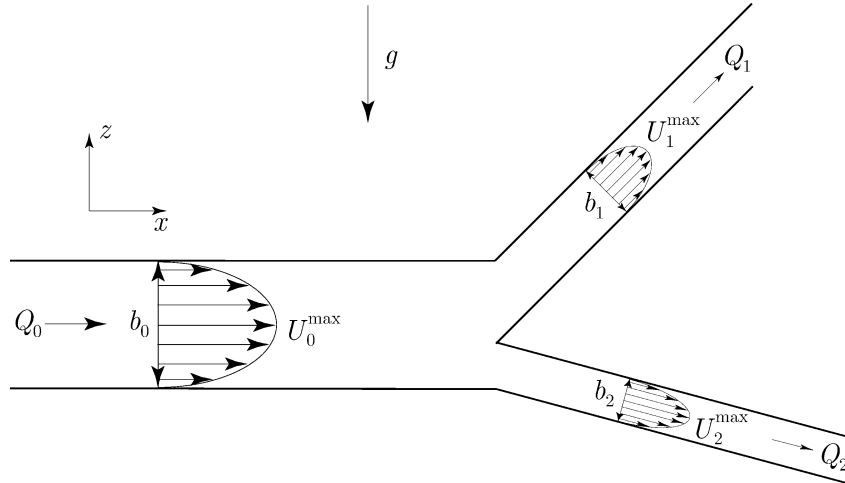


Fig. 1. Schematic illustration of the bifurcating fracture considered in this study.

fracture system. This is a reasonable assumption if hydraulic conductivities in the surrounding matrix are several orders of magnitude lower than conductivity within the fracture [1].

A uniform pressure gradient imposed on the bifurcating fracture induces flow in the parent fracture. The volumetric flow rate per unit fracture depth is the product of the mean flow velocity and the fracture aperture. The fluid is considered incompressible; therefore the sum of the volumetric flow rates into the daughter fractures must equal the flow rate out of the parent fracture,

$$Q_0 = Q_1 + Q_2. \quad (1)$$

In the notation for this work, subscript 0 refers to the parent fracture, and subscripts 1 and 2 refer to daughter fractures one (upper) and two (lower), respectively. All flows within the system are specified by stipulating a maximum centerline velocity in the parent fracture,  $U_0^{\max}$ , along with the aperture of the parent,  $b_0$ , and flow rates in each daughter fracture,  $Q_1$  and  $Q_2$  such that (1) is upheld.

## 2.2. Dense colloid transport

The transport of colloids in bifurcating fractures is simulated with a particle tracking algorithm. A plume of particles is injected instantaneously at the entrance of the parent fracture ( $x_0 = 0$ ) at time zero. Particles are assigned initial  $z_0$  coordinates in proportion to the local flow rate such that they are wholly contained within the fracture with no particle–wall overlap [3,7]. Colloids neither diffuse into the fracture matrix nor attach onto the fracture wall and when a colloid encounters a wall, it is reflected back into the fracture without loss of energy. If dense colloids ( $> 1000 \text{ kg/m}^3$ ) are considered, the effects of gravitational settling must be incorporated into the particle tracking equations [4],

$$x^m = x^{m-1} + u(x^{m-1}, z^{m-1})\Delta t + U_s \Delta t + Z(0, 1)\sqrt{2\mathcal{D}_{d_p}}\Delta t, \quad (2)$$

$$z^m = z^{m-1} \pm \Delta z, \quad (3)$$

where  $u(x, z)$  is the local Poiseuille fluid velocity;  $Z(0, 1)$  is a random selection from the standard normal distribution; and  $m$  is the spatial step level. Because of the low velocities modeled here, particle motion due to shear effects is neglected. The molecular diffusion coefficient for a spherical particle is inversely proportional to its diameter,  $d_p$ , according to the Stokes–Einstein diffusion equation,

$$\mathcal{D}_{d_p} = \frac{kT}{3\pi\eta d_p}, \quad (4)$$

where  $k$  is Boltzmann’s constant,  $T$  is the absolute temperature, and  $\eta$  the dynamic viscosity of the interstitial fluid. The local parabolic velocity profile within each fracture is expressed as

$$u(x, z) = U_0^{\max} \left[ 1 - 4 \left( \frac{z}{b_0} \right)^2 \right]. \quad (5)$$

The settling velocity is included in the particle tracking equations as an additional deterministic velocity and for a small spherical particle is given as

$$U_s = -\frac{(\rho_p - \rho_f)gd_p^2}{18\eta}, \quad (6)$$

where  $\rho_f$  and  $\rho_p$  are the densities of the suspending fluid and the colloids, respectively, and  $g$  is the acceleration due to gravity in the negative  $z_0$ -direction.

A constant-time-step particle-tracking algorithm is ill suited to simulate colloid plumes of varying diameters because the accuracy of such an algorithm is dependent upon maintaining a small, consistent displacement at each time step. Subject to a constant time step, small colloids travel quite differently than large colloids due to both gravitational and diffusive effects. A constant spatial step particle tracking algorithm is a better choice. The time necessary for a dense colloid to move a specified spatial step in the  $z$ -direction is necessarily affected by gravitational settling. Upon selection of a spatial step, a random time step for plumes subject to gravitational settling is generated from the solution to the

equation ([8], Eq. 15):

$$\Delta z = U_s \Delta t \pm \sqrt{\tau \mathcal{D}_{d_p} \Delta t}, \quad (7)$$

where  $\tau$  is dimensionless time ([9], Eq. 13),

$$\tau = \frac{(\Delta z)^2}{\mathcal{D}_{d_p} \Delta t} = 2.656 \exp[-0.787Z(0, 1)]. \quad (8)$$

Substituting (8) into (7) and rearranging yields the following quadratic equation for  $\Delta t$  ([8], Eq. 17):

$$\Delta t = \frac{U_s \Delta z + 1.328 \exp[-0.787Z(0, 1)] \mathcal{D}_{d_p}}{U_s^2} \pm \frac{\sqrt{(U_s \Delta z + 1.328 \exp[-0.787Z(0, 1)] \mathcal{D}_{d_p})^2 - U_s^2 (\Delta z)^2}}{U_s^2}. \quad (9)$$

The positive root of (9) gives the time required to move the fixed distance increment if the diffusive displacement is opposite gravitational settling, and the negative root gives the time increment if the diffusive displacement is in the same direction as gravitational settling. The root of  $\Delta t$ , and therefore the sign of  $\Delta z$  in (3), is determined from a random number uniformly distributed between zero and one (negative if less than or equal to 0.5, positive if greater than 0.5). Lighter than water colloids may be similarly considered if desired.

### 2.3. Bifurcation

At the bifurcation, the ratio of the daughter fracture flow rates (per unit depth) is used to determine which daughter fracture a particle enters. The  $z_0$ -location of the streamline in the parent fracture that terminates at the stagnation point between the two daughter fractures at the bifurcation is determined by equating the flow rate (per unit depth) of daughter fracture 2 with the equivalent flow rate from a portion of the parent parabolic velocity profile,

$$\int_{-b_0/2}^{z_0} U_0^{\max} \left[ 1 - 4 \left( \frac{z}{b_0} \right)^2 \right] dz = Q_2. \quad (10)$$

Evaluating the integral yields the following cubic equation of reduced form in  $z_0$ ,

$$U_0^{\max} z_0 \left[ 1 - \frac{4}{3} \left( \frac{z_0}{b_0} \right)^2 \right] + \frac{Q_0}{2} - Q_2 = 0, \quad (11)$$

which has one real root at the stagnation point.

During the spatial step that a colloid moves from the parent fracture to a daughter fracture, its last  $z_0$  coordinate is used to determine which daughter fracture the colloid enters. If  $z_0$  is less than the solution to Eq. (11), the colloid enters daughter fracture 2 (and daughter fracture 1 if greater). For neutrally buoyant colloids, routes are determined according to the relative quantities of fluid flow in each of the daughter fractures. Intuitively, neutrally buoyant colloids are obliged to enter a daughter fracture in proportion to flow

rates. The number of colloids entering each daughter fracture are counted and the ratio,  $R$ , of colloids in daughter fracture 1 to daughter fracture 2 is determined. The ratio,  $R$ , is used as a metric to evaluate how characteristic times impact the selection of a daughter fracture. When this ratio approaches unity, it implies that there is no preference for one fracture over another. As it approaches zero, it means that virtually all colloids enter daughter fracture 2 due to gravitational effects. This ratio can be multiplied by the flow rate ratio to find how colloids partition in daughter fractures of any aperture. For clarification, consider a system comprising a parent fracture with flow  $Q_0 = 6.67 \times 10^{-11} \text{ m}^3/\text{s}$  that bifurcates into daughter fractures with flow rates  $Q_1 = 5.14 \times 10^{-11} \text{ m}^3/\text{s}$  and  $Q_2 = 1.52 \times 10^{-11} \text{ m}^3/\text{s}$ . For this system,  $Q_1 = 3.38Q_2$ . If the ratio of daughter fracture colloids for a particular simulation were  $R = 0.75$ , this would yield  $0.75 \times 3.38 = 2.54$  times as many colloids entering daughter fracture 1 as daughter fracture 2.

### 2.4. Characteristic times

Three characteristic times, advective, settling, and diffusive, dictate how colloids partition at a bifurcation. They are defined here as

$$t_{\text{adv}} = \frac{3x_0}{2U_0^{\max}}, \quad (12)$$

$$t_{\text{set}} = \frac{b_0}{U_s}, \quad (13)$$

$$t_{\text{diff}} = \frac{b_0^2}{2\mathcal{D}_{d_p}}, \quad (14)$$

respectively. The selection of the appropriate daughter fracture is related to the relative values of the advective, settling, and diffusive characteristic times. Ultimately, it is the ratios of these characteristic times that dictate which fracture the colloids will enter and what their overall residence times will be.

## 3. Simulations and discussion

Three parameters,  $\Delta\rho = \rho_p - \rho_f$ ,  $d_p$ , and  $U_0^{\max}$ , are incrementally varied with ranges shown in Table 1. The ranges of model parameters used in these simulations were selected to be consistent with values that might be expected in natural subsurface media. The length of the parent fracture considered in this work is 1 m with constant aperture,  $b_0 = 1 \times 10^{-4} \text{ m}$ . For the particle tracking simulations performed here, daughter fractures are assigned equal flow rates,  $Q_1 = Q_2$ . Plumes of 1000 colloids are instantaneously released into the parent fracture for all simulations. Characteristic times and ratios of colloids entering the daughter fractures are calculated for each plume.

The spread of  $R$  as it approaches unity is due to the Monte Carlo nature of the 1000 particle random-walk technique. Using more particles would decrease the random

Table 1  
Daughter fracture parameter values for model simulations

Parameter	Minimum	Maximum	Increment
$\Delta\rho$ (kg/m <sup>3</sup> )	10	1000	10
$d_p$ (m)	$1 \times 10^{-8}$	$1 \times 10^{-6}$	$1 \times 10^{-8}$
$U_0^{\max}$ (m/s)	$1 \times 10^{-7}$	$1 \times 10^{-5}$	$1 \times 10^{-7}$

noise, but increase computational cost. Several informative results can be inferred from plots of  $R$  against the ratio of characteristic times. Fig. 2a shows how  $R$  changes as the ratio of  $t_{\text{set}}/t_{\text{diff}}$  and Fig. 2b illustrates how  $R$  changes with  $t_{\text{set}}/t_{\text{adv}}$ . In Fig. 2a there are several noteworthy observations: (a) when the  $t_{\text{set}} \lesssim 0.1t_{\text{diff}}$  virtually all colloids enter daughter fracture 2 due to gravitational effects; (b) when the  $t_{\text{set}} \approx t_{\text{diff}}$  twice as many colloids enter daughter fracture two than daughter fracture one,  $R = 0.5$ ; and, (c) when the  $t_{\text{set}} \gtrsim 10t_{\text{diff}}$  colloids are unaffected by gravity and partition equally between daughter fractures. In Fig. 2b, (a) when the  $t_{\text{set}} \lesssim 10^{-4}t_{\text{adv}}$  colloid transport is dominated by gravitational effects and they enter fracture 2; (b) when the  $10^{-3}t_{\text{set}} \lesssim t_{\text{adv}} \lesssim 10^{-2}t_{\text{set}}$  plume partitioning between daughter fractures can vary greatly; and, (c) when the  $t_{\text{set}} \gtrsim 0.1t_{\text{adv}}$  colloids are unaffected by gravity and partition equally between daughter fractures. The reason for this wide range of partition ratios over such a wide range of characteristic times ratios for case (b) is because  $t_{\text{adv}}$  is a constant, independent of colloid size. However, the average advection time of a colloid plume is affected by the particle size because dense particles tend to sink to the bottom of the parent fracture and assume the slower moving velocities of the parabolic profile found there. Therefore, there is a wide range of ratios of characteristic settling to advection times that allow the colloids either to remain unaffected by gravity or to predominantly enter daughter fracture 2. Transition zones lie on either side of the above-specified range. That is, for  $10^{-4}t_{\text{set}} \lesssim t_{\text{adv}} \lesssim 10^{-3}t_{\text{set}}$  colloids are in-

creasingly affected by gravity, and conversely for  $10^{-2}t_{\text{set}} \lesssim t_{\text{adv}} \lesssim 0.1t_{\text{set}}$ .

#### 4. Conclusion

A bifurcating fracture system comprising a parent fracture dividing into two daughter fractures is used to examine the transport of colloids. Neutrally buoyant colloids partition between daughter fractures in proportion to the flow rates. When dense colloids are used, particles preferentially enter daughter fracture 2. The ratios of characteristic advective, settling, and diffusive times dictate which fracture colloids tend to enter. If the characteristic time for settling in the entrance fracture is more than an order of magnitude less than the characteristic time for advection or the characteristic settling time is more than an order of magnitude greater than the characteristic diffusion time, then colloids will be unaffected by gravity and will partition according to volumetric flow rates between the exit fractures. Nearly all of the colloids will enter daughter fracture 2 if diffusion time is an order of magnitude greater than the settling time or the advection time is more than four orders of magnitude greater than the settling time. There is a transition range, especially for ratios of characteristic settling to characteristic advection times, where the size of the colloids and their density dictate how they partition.

#### Acknowledgments

Sandia is a multiprogram laboratory operated by Sandia Corporation, a Lockheed Martin company, for the United States Department of Energy under Contract DE-AC04-94AL85000. Special thanks to Dr. Paul Reimus for his insightful comments and suggestions.

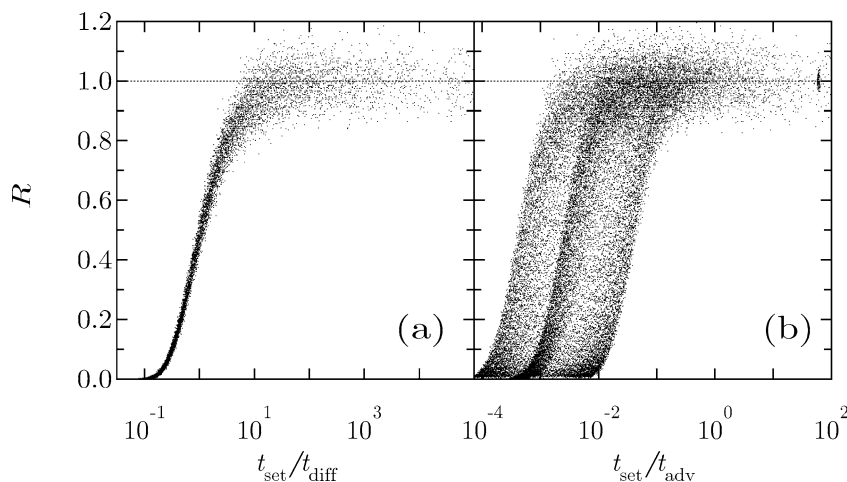


Fig. 2. Variation of  $R$  with ratios of characteristic times: (a) illustrates how  $R$  changes as a function of the ratio of characteristic settling to diffusive times, and (b) shows how  $R$  is a function of the ratio of characteristic settling to advective times. The dashed line indicates  $R = 1$ .

**References**

- [1] A. Abdel-Salam, C.V. Chrysikopoulos, *Water Resour. Res.* 32 (6) (1996) 1531–1540.
- [2] S.C. James, C.V. Chrysikopoulos, *Water Resour. Res.* 35 (3) (1999) 707–718.
- [3] S.C. James, C.V. Chrysikopoulos, *Water Resour. Res.* 36 (6) (2000) 1457–1465.
- [4] C.V. Chrysikopoulos, S.C. James, *Transp. Por. Media* 51 (2003) 191–210.
- [5] S.C. James, C.V. Chrysikopoulos, *Colloids Surf.* 226 (1–3) (2003) 101–118.
- [6] S.C. James, C.V. Chrysikopoulos, *J. Colloid Interface Sci.* 263 (2003) 288–295.
- [7] P.W. Reimus, *The Use of Synthetic Colloids in Tracer Transport Experiments in Saturated Rock Fractures*. Ph.D. thesis, LA-13004-T, Los Alamos National Laboratory, 1995.
- [8] P.W. Reimus, S.C. James, *Chem. Eng. Sci.* 57 (21) (2002) 4429–4434.
- [9] S.C. James, C.V. Chrysikopoulos, *Chem. Eng. Sci.* 56 (23) (2001) 6535–6543.